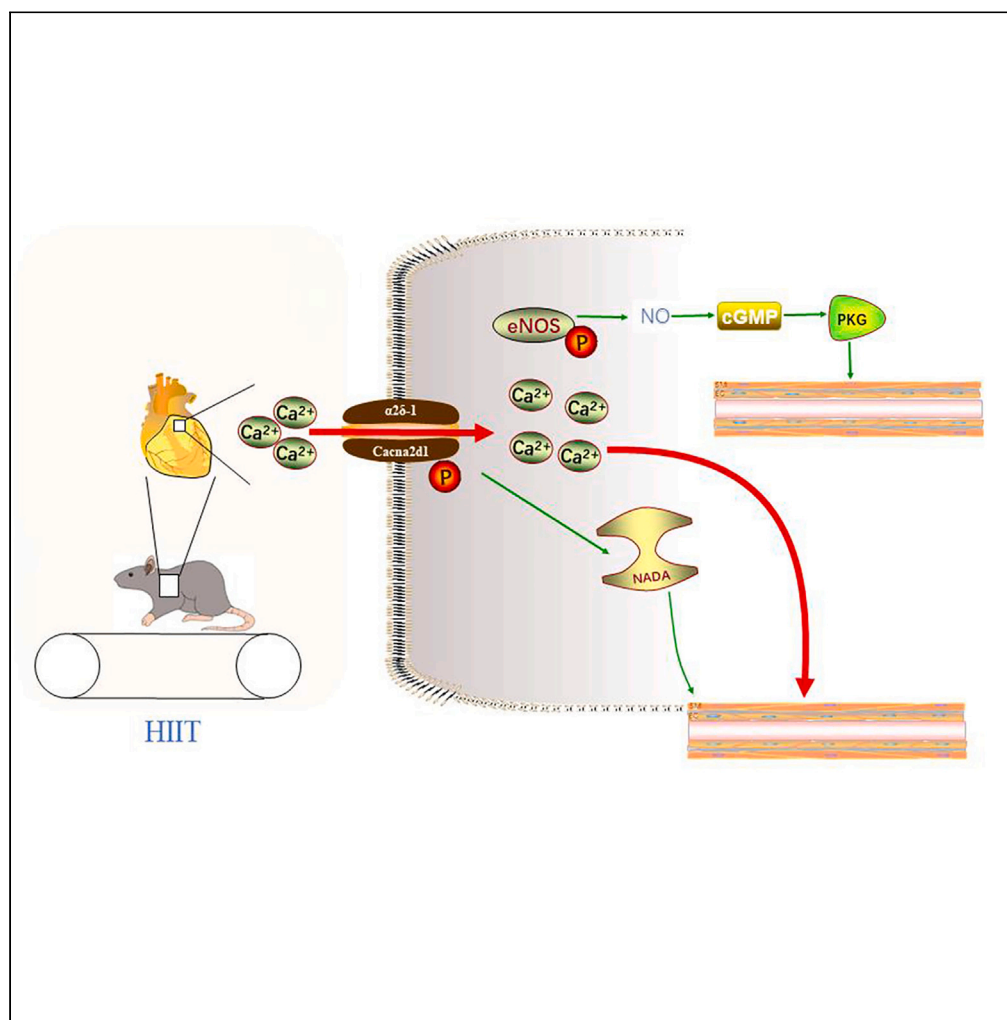


Article

Exercise training affects calcium ion transport by downregulating the CACNA2D1 protein to reduce hypertension-induced myocardial injury in mice



Shan Gao, Wei Yao, Rui Zhou, Zuwei Pei

pzw_dl@163.com

Highlights

Ca²⁺ concentration increase can induce LAMA2 aggregation

High concentration of Ca²⁺ can promote the activity of ITGA7

HIIT can treat HTN in mice compared to MICT by downregulating CACNA2D1

Downregulating CACNA2D1 reduces Ca²⁺ concentration, improving myocardial damage

Gao et al., iScience 27, 109351
April 19, 2024 © 2024 The Author(s).
<https://doi.org/10.1016/j.isci.2024.109351>



Article

Exercise training affects calcium ion transport by downregulating the CACNA2D1 protein to reduce hypertension-induced myocardial injury in mice

Shan Gao,¹ Wei Yao,² Rui Zhou,² and Zuowei Pei^{1,3,4,5,*}

SUMMARY

Hypertension is a risk factor for cardiovascular disease, and exercise has cardioprotective effects on the heart. However, the mechanism by which exercise affects hypertension-induced myocardial injury remains unclear. Exercise response model of hypertension-induced myocardial injury in mice was analyzed using multiomics data to identify potential factors. The study found that serum Ca²⁺ and brain natriuretic peptide concentrations were significantly higher in the HTN (hypertension) group than in the control, HTN+MICT (moderate intensity continuous exercise), and HTN+HIIT (high intensity intermittent exercise) groups. Cardiac tissue damage and fibrosis increased in the HTN group, but exercise training reduced pathological changes, with more improvement in the HTN+HIIT group. Transcriptomic and proteomic studies showed significant differences in CACNA2D1 expression between the different treatment groups. HIIT ameliorated HTN-induced myocardial injury in mice by decreasing Ca²⁺ concentration and diastolizing vascular smooth muscle by downregulating CACNA2D1 via exercise.

INTRODUCTION

Hypertension is a widespread disease worldwide and can be divided into primary and secondary hypertension. Primary hypertension is a syndrome, not a disease, but various etiologies have common signs such as elevated blood pressure.¹ However, current research shows that the vast majority of patients with hypertension have not yet found the cause of their hypertension and have secondary hypertension.² Approximately 5%–10% of patients with hypertension have secondary hypertension, which is primarily caused by renal parenchyma disease, renal vascular hypertension, and primary hyperaldosteronism.^{2,3} In the traditional sense, hypertension refers to blood pressure $\geq 140/90$ mmHg, whereas normal blood pressure is often 120/80 mmHg.⁴ Hypertension is one of the most common circulatory diseases and accounts for over 40% of all cardiovascular diseases.⁵ Hypertension is the leading cause of myocardial infarction and stroke worldwide. Furthermore, hypertension can cause serious lesions in the heart, blood vessels, kidneys, eyes, brain, and other organs.⁶ The main contributing factor to hypertension is cardiovascular autonomic dysfunction, characterized by sympathetic overactivity,⁷ as well as endothelial dysfunction, increased oxidative stress, vascular abnormalities, and other factors.⁸ Studies have shown that, as a slow-moving disease, arterial hypertension affects 40% of the population worldwide and has a high incidence in the elderly.⁹ With the dietary and/or behavioral changes today, hypertension has become increasingly common, and its prevalence is high, showing a gradual increase.^{10,11} A characteristic pathological change in the development of hypertension is an increase in voltage-dependent Ca²⁺ inward flow in vascular smooth muscle cells.¹² Therefore, the active search for methods and related mechanisms to prevent, treat, manage, and control hypertension is extremely important for human health.

Drugs are mainly used to control blood pressure in the treatment of hypertension, although an increasing number of studies have shown that people with hypertension engage in less physical exercise than those without hypertension, and regular exercise can reduce hypertension, especially in people with hypertension.¹³ Exercise improves vascular smooth muscle cell contractility by modulating voltage-gated calcium channels (Cav).¹⁴ Cav belongs to the class of calcium channels, mainly distributed in cardiac muscle, skeletal muscle, and other parts of the basic molecular structure by the formation of ion channels of the main subunit $\alpha 1$ and auxiliary subunits $\alpha 2$, β , δ , and γ composed of pentameric proteins. Cav can be divided into three major categories of Cav1, Cav2, and Cav3 from the homology of genes, and each of these categories is divided into a number of isoforms according to the genes coding for the $\alpha 1$ subunit.¹⁵ Among them, the $\alpha 2\delta$ -1 subunit is encoded by the CACNA2D1 gene, which is expressed at a high level in skeletal muscle, cardiac vascular smooth muscle, and the brain.¹⁶ Regular physical exercise has also been proven effective in reducing blood pressure in

¹Department of Central Laboratory, Central Hospital of Dalian University of Technology, Dalian, China

²Department of Internal Medicine, The Affiliated Zhong Shan Hospital of Dalian University, Dalian, China

³Department of Cardiology, Central Hospital of Dalian University of Technology, Dalian, China

⁴Faculty of Medicine, Dalian University of Technology, Dalian, China

⁵Lead contact

*Correspondence: pzw_dl@163.com

<https://doi.org/10.1016/j.isci.2024.109351>



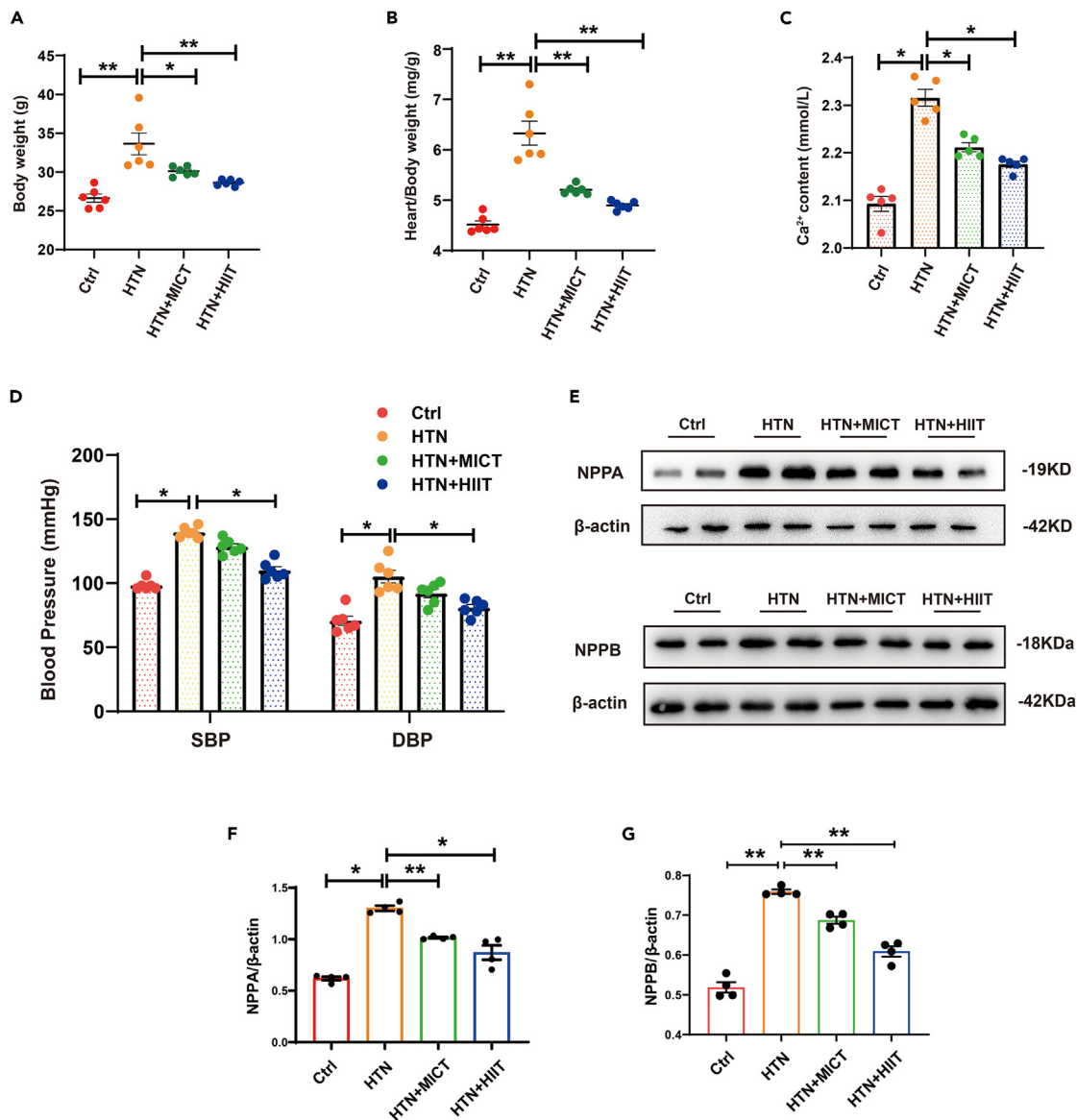


Figure 1. Metabolic data from the different groups were processed differently for 22 weeks

(A and B) Quantitative analysis of body weight and heart/body weight in each group. Each group is n = 6. Compared with HTN group, *p < 0.05; Compared with HTN group, **p < 0.01.

(C) Ca²⁺ levels in each group. Each group is n = 6. Compared with HTN group, *p < 0.01.

(D) Blood Pressure levels in each group. Each group is n = 6. Compared with HTN group, *p < 0.01.

(E–G) Representative western blot images showing the expression of NPPA and NPPB in cardiac tissues. Data are expressed as mean ± SEM; Each group is n = 4. Compared with HTN group, *p < 0.05; Compared with HTN group, **p < 0.01.

patients with hypertension.¹⁰ Furthermore, taking antihypertensive drugs in addition to appropriate physical exercise can further control high blood pressure.⁶ For the reduction and control of blood pressure, different exercise treatments, such as aerobic exercise and resistance training, have different effects, which is important for further exploration of the mode and intensity that are the best choices for the reduction of blood pressure.¹⁷ Although a large amount of evidence suggests that exercise can reduce blood pressure in patients with hypertension, little is known about the related mechanisms involved.^{6,9} Furthermore, the proportion of patients with hypertension participating in exercise is very small.¹⁸ Some researchers have focused on microRNAs (miRNAs) and found that there was no change in the expression of miRNA-214 in non-hypertensive animals receiving exercise training, whereas miRNA expression in trained hypertensive animals was high.¹⁹ The regulatory mechanism of exercise in hypertension, especially the protein and gene regulatory sites involved, remains unclear.

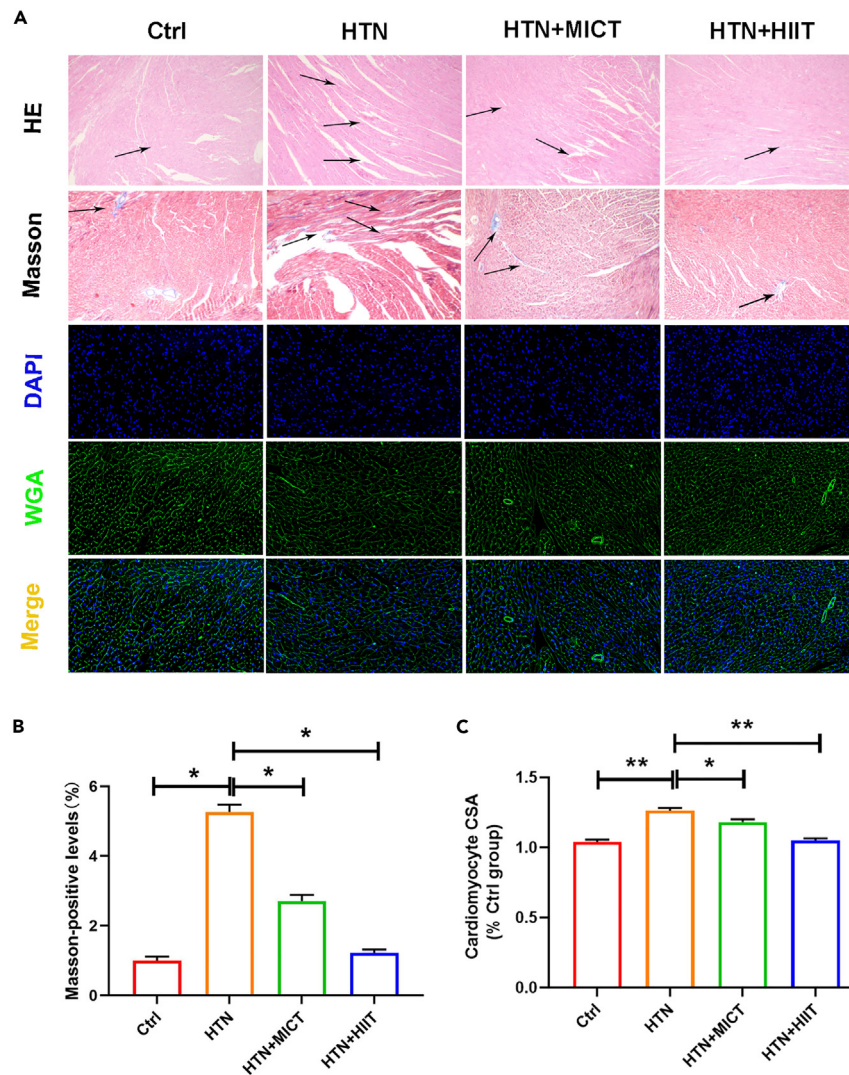


Figure 2. Histopathological changes of different exercise intensity training on hypertension-induced myocardial injury in mice

(A) H&E, Masson, and WGA staining of heart tissue sections at magnification 40 \times . The arrows indicate positive stained cells.

(B) Masson's trichromatic staining quantitative analysis in each group. Data are given as mean \pm SEM; Each group is n = 3. *p < 0.05 vs. the HTN group.

(C) WGA staining showed quantitative analysis of cardiomyocyte CSA. Data are given as mean \pm SEM; Each group is n = 3. *p < 0.05 vs. the HTN group; **p < 0.01 vs. the HTN group.

Therefore, we speculate that exercise may play a regulatory role in hypertension because it changes the expression of certain genes and proteins in the body.

RESULTS AND DISCUSSION

Metabolic characterization

The metabolic characteristics of the four groups of mice after exercise treatment are shown in Figure 1. Body weight and heart/body weight ratio were significantly lower in the control, HTN+MICT (hypertension + moderate intensity continuous exercise), and HTN+HIIT (hypertension + high intensity intermittent exercise) groups than in the HTN group (Figures 1A and 1B). Systolic blood pressure (SBP) and diastolic blood pressure (DBP) were significantly lower in the control, HTN+MICT, and HTN+HIIT groups than in the HTN group (Figure 1D). Blood pressure markers, such as Ca²⁺ concentration, increased significantly in the HTN group, decreased in the exercise therapy group, and decreased significantly in the HTN+HIIT group. (Figure 1C). Natriuretic peptide precursor A (NPPA) and NPPB were detected by WB to evaluate indicators of cardiac function in mice. The results showed that the expression of NPPA and NPPB in the HTN+MICT and HTN+HIIT groups was significantly lower than that in the HTN group, and the expression of the HTN+HIIT group was lower than that of the HTN+MICT group. (Figures 1E–1G).

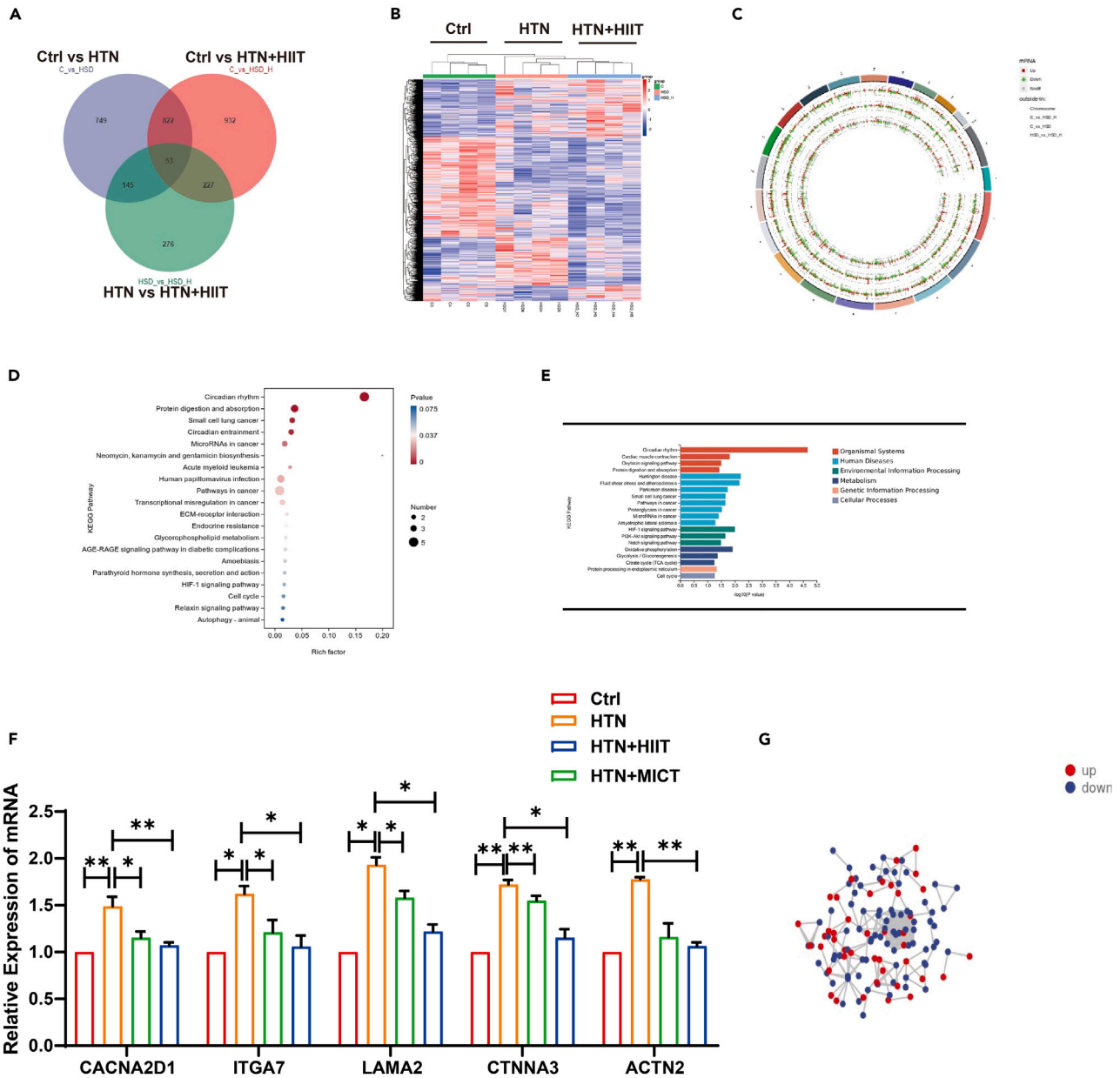


Figure 3. mRNA levels in hypertension-induced myocardial injury mice

(A) Venn diagram analysis of three groups of mice.

(B) Heatmaps in the heart tissues of different groups of mice.

(C) Genetic circle map analysis of three groups of mice.

(D) Bubble chart analysis of three groups of mice.

(E) KEGG analysis in three groups of mice.

(F) Relative Expression of CACNA2D1, ITGA7, LAMA2, CTNNA3, and ACTN2. Data are given as mean \pm SEM; Each group is n = 4. *p < 0.05 vs. the HTN group;

**p < 0.01 vs. the HTN group.

(G) The relationship between significantly upregulated and downregulated genes.

Histopathological changes in cardiac tissues

Hematoxylin and eosin (H&E), Masson's trichrome, and fluorescein isothiocyanate (FITC)-conjugated wheat germ agglutinin (WGA) staining were used to measure cardiac tissue damage (Figure 2). H&E and WGA staining revealed cardiomyocyte hypertrophy and inflammatory cell infiltration. Compared to the control group, myocardial hypertrophy was observed, and the cardiomyocyte cross-sectional area (CSA)

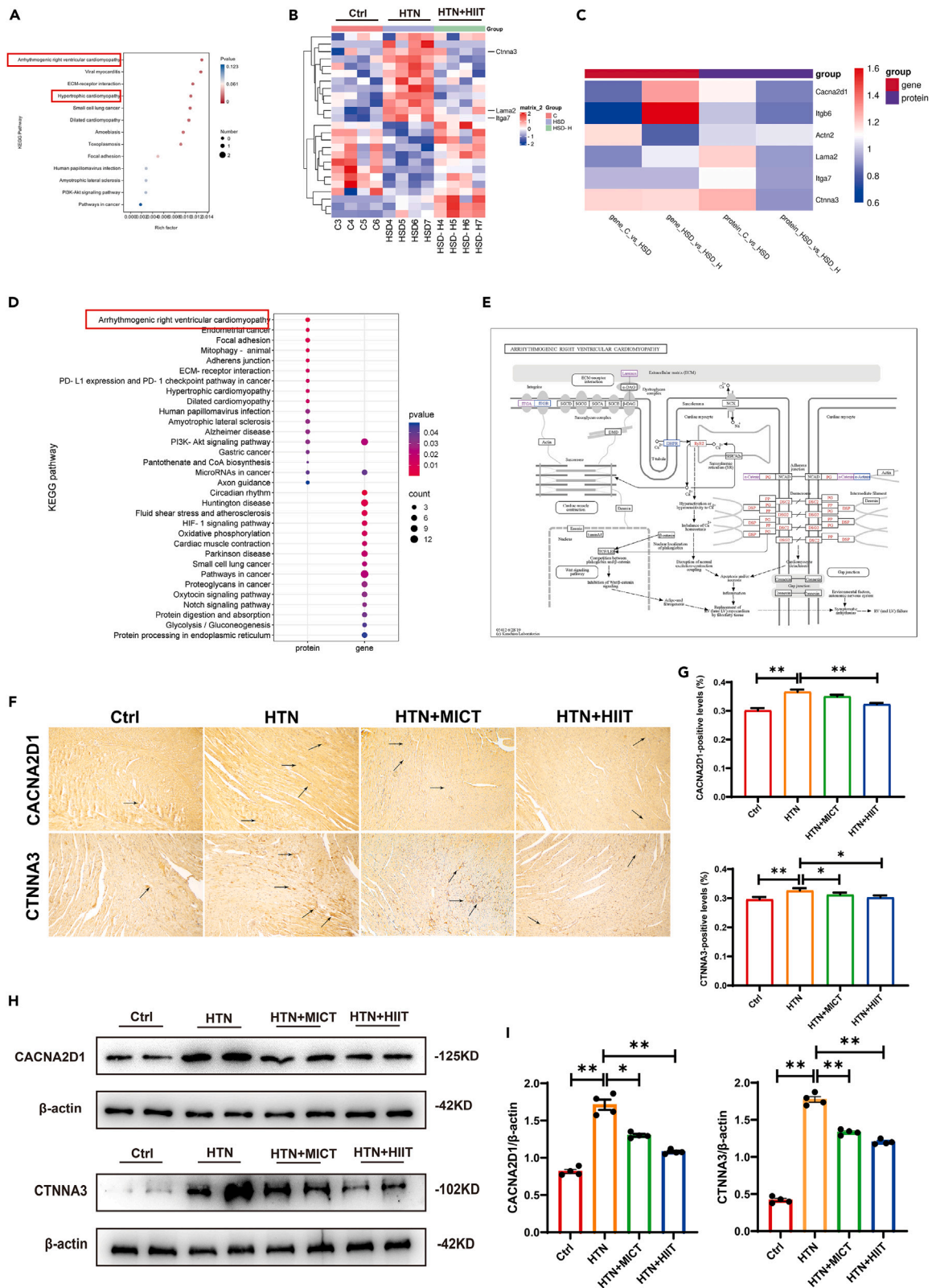


Figure 4. HIIT reduced Ca^{2+} content in mice with HTN-induced myocardial injury

(A) Bubble chart analysis of three groups of mice.

(B and C) Heatmaps in the heart tissues of different groups of mice.

(D) KEGG enrichment analysis results (HTN group vs. HTN+HIIT group).

(E) Pathway of arrhythmogenic right ventricular cardiomyopathy.

(F) Representative immunohistochemistry images showing the expression of CACNA2D1 and CTNNA3 in myocardial tissue. Magnification 10 \times ; The arrows illustrate areas with stained cells.

(G) Quantification of the CACNA2D1 and CTNNA3 expression levels. Data are expressed as mean \pm SEM; n = 3, *p < 0.05 vs. HTN group, **p < 0.01 vs. HTN group.

(H and I) Representative western blot images showing the expression of CACNA2D1 and CTNNA3 in cardiac tissues. Data are expressed as mean \pm SEM; n = 4, *p < 0.05 vs. HTN group, **p < 0.01 vs. HTN group.

increased in the HTN group. However, the levels of tissue damage factors decreased in the HTN+MICT and HTN+HIIT groups and improved significantly in the HTN+HIIT group.

Transcriptomic analysis of cardiac tissue of hypertension-induced myocardial damage after exercise training in mice

The previous results show that HIIT had a more significant therapeutic effect than MICT in mice with hypertension-induced myocardial injury. To investigate the factors that affect HTN-induced myocardial injury in mice during exercise training, we performed RNA sequencing (RNA-seq). We analyzed differentially expressed genes among mice in the control, HTN, and HTN+HIIT groups (Figure 3A). Figure 3B shows a heatmap of genes related to cardiovascular disease identified by microarray screening. Genogram and Kyoto Encyclopedia of Genes and Genomes (KEGG) analysis of the RNA-seq data showed significant differences in the expression of cardiovascular-related genes in the control, HTN, and HTN+HIIT groups (Figures 3C–3E). Exercise training has been suggested to play an important role in the regulation of the whole process of cardiovascular disease.

Based on transcriptomic analysis of the mRNA expression levels of cardiovascular-related genes, we studied the Ca^{2+} channel protein-related gene CACNA2D1 in mice with hypertension-induced myocardial injury. CACNA2D1 expression was significantly higher in the HTN group than in the control group, whereas it was significantly lower in the HTN+HIIT group than in the HTN group. Figure 3F showed the expression levels of Lamin subunit α -2 (LAMA2), catenin α -3 (CTNNA3), and genetic variants in α -actinin-2 (ACTN2) in cardiac tissues of the different groups of mice. The expression of CACNA2D1, integrin (ITGA7), LAMA2, CTNNA3, and ACTN2 was verified using qPCR. These results were consistent with histological results, and the expression levels of the five genes were all lower than those of the HTN group after exercise (Figure 3F). The relationship between significantly upregulated and downregulated genes was also determined by the results of gene and protein interaction (Figure 3G).

HIIT decreased Ca^{2+} content in mice with HTN-induced myocardial injury

According to the results of the proteomics analysis, we determined that the signaling pathway dominated by arrhythmic right ventricular cardiomyopathy changed in the HIIT+HTN and HTN groups (Figures 4A–4E). Therefore, we performed immunohistochemical and western blot analyses to verify the involvement of CACNA2D1 and CTNNA3 in this pathway. Immunohistochemistry (Figures 4F and 4G) and western blot (Figures 4H and 4I) were performed to assess the levels of Ca^{2+} channel protein-related indicators. Western blot and immunohistochemistry showed that HTN+HIIT decreased the expression levels of CACNA2D1 and CTNNA3 compared to those in the HTN group and HTN+MICT group.

HIIT improves hypertension-induced myocardial injury in mice by reducing calcium transport channel-associated proteins

Western blot was performed to determine the levels of calcium ion-related indicators. LAMA2 is a protein widely expressed in vascular endothelial cells and smooth muscle cells. Integrin α -7 (ITGA7) can regulate the contraction and relaxation of cardiomyocytes. ACTN2 gene is related to calcium ion transport; its expression assists calcium ion transport and then affects the contraction and relaxation function of the heart, with the expressed protein being α -actinin. Western blot images showed that, compared to the HTN group, the expression levels of LAMA2, α -actinin, and ITGA7 in HTN+HIIT group decreased (Figures 5A–5F). The expression levels of LAMA2, α -actinin, and ITGA7 in the HTN+HIIT group were lower than those in the HTN group and HTN+MICT group.

HIIT ameliorates hypertension-induced myocardial injury in mice via the eNOS-NO-cGMP-PKG pathway

Western blot was used to assess the levels of eNOS (endothelial nitric oxide synthase)-NO-cGMP (cyclic guanosine monophosphate)-PKG (cGMP-dependent protein kinase G)-related indicators. HTN+HIIT increased the expression levels of PKG and eNOS compared to those in the HTN group and HTN+MICT group (Figures 6A and 6B). Phosphorylation of PDE5 can activate its enzymatic activity, improve its affinity for cGMP binding in the regulatory domain, and reduce the intracellular levels of cGMP. By testing the expression of PDE5, it was highly expressed in the HTN group, but decreased in the HTN+HIIT group (Figures 6C and 6D), indicating that the cGMP level in the HTN+HIIT group was higher than that in the HTN group and HTN+MICT group.

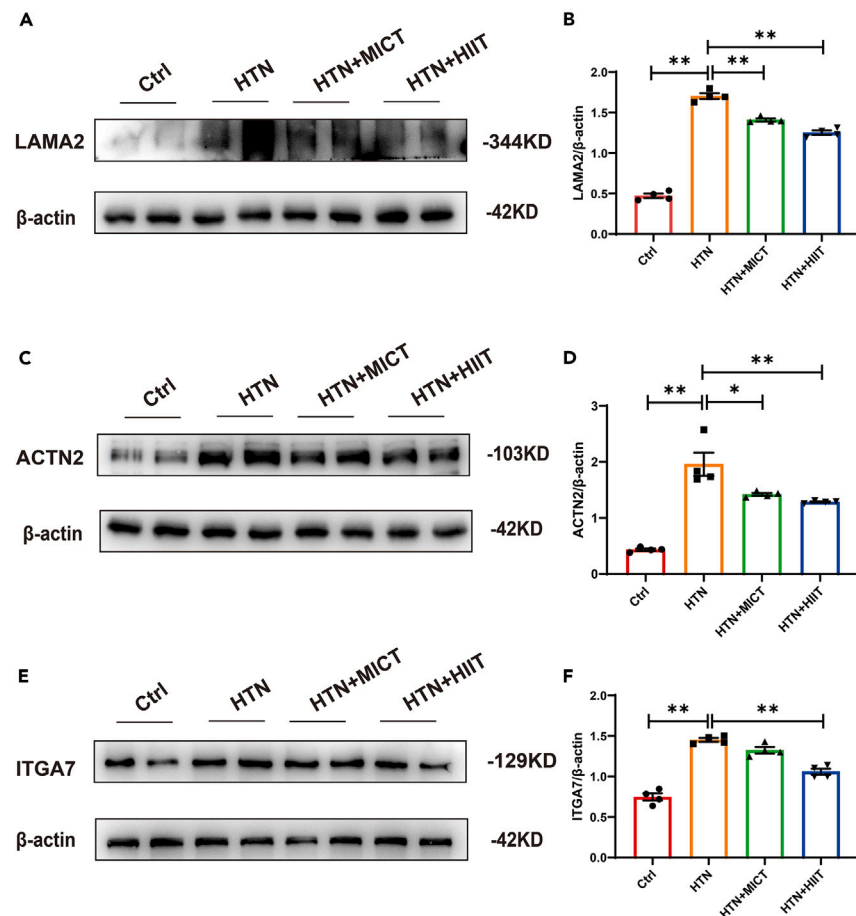


Figure 5. HIIT improves myocardial damage induced by hypertension in mice by reducing calcium transport channel-associated proteins

(A and B) Representative western blot images showing the expression of LAMA2 in cardiac tissues. Data are expressed as mean \pm SEM; n = 4, *p < 0.05 vs. HTN group, **p < 0.01 vs. HTN group.

(C and D) Representative western blot images showing the expression of ACTN2 in cardiac tissues. Data are expressed as mean \pm SEM; n = 4, *p < 0.05 vs. HTN group.

(E and F) Representative western blot images showing the expression of ITGA7 in cardiac tissues. Data are expressed as mean \pm SEM; n = 4, *p < 0.05 vs. HTN group.

Downregulating CACNA2D1 regulated Angiotensin II (Ang II)-treated myocardial microvascular endothelial cells (MCMECs)

As shown in Figure 7A, MCMEC induced by 10 μ mol/L Ang II could induce cell proliferation after 48 h, but there was no significant change after 24 h. The MCMEC was transfected with small interfering RNA (siRNA) CACNA2D1 and siRNA negative control and tested by western blot. The expression of CACNA2D1 protein in MCMEC in the CACNA2D1 silencing group was significantly lower than that in the control group (Figures 7B and 7C). CD31 and CACNA2D1 immunofluorescence double staining was performed on the paraffin sections of the left heart tissue of four groups of mice. The results showed that CD31 and CACNA2D1 were colocalized in the left cardiac tissue of mice. The expression of CACNA2D1 in endothelial cells in the HTN group was higher than that in the control group. The expression intensity of CACNA2D1 in HTN+HIIT group was lower than that of HTN+MICT in endothelial cells (Figure 7D). Western blot analysis was performed to detect the changes of related protein levels in MCMEC under different treatments. The results indicated that downregulating CACNA2D1 could improve the MCMEC of Ang II treatment (Figures 7E and 7F).

Downregulating CACNA2D1 can improve MCMEC injury induced by Ang II

Western blot detection of correlation between different treatments of MCMEC protein level expression changes was carried out. The experimental results showed that the protein levels of LAMA2, ACTN2, and ITGA7 in the siRNA+Ang II group were lower than those in the siRNA group, and the protein levels were higher than those in the siRNA group (Figures 8A–8C), indicating that downregulating CACNA2D1 could improve the MCMEC treated with Ang II. Further verification results showed that downregulating CACNA2D1 in the eNOS-NO-cGMP-PKG pathway could protect Ang II-treated MCMEC (Figures 8D and 8E).

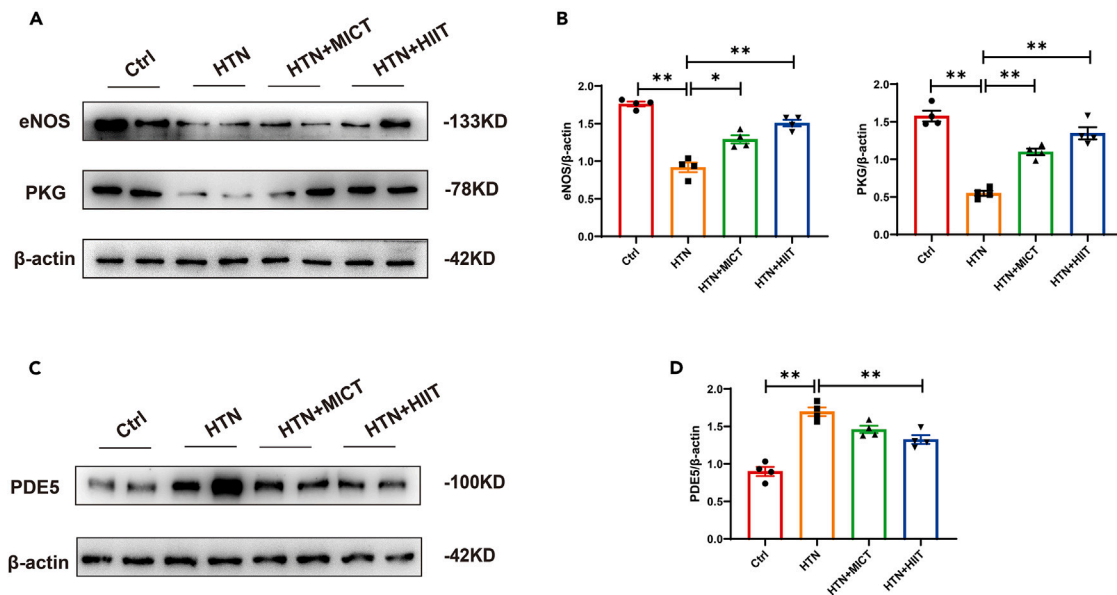


Figure 6. HIIT ameliorates hypertension-induced myocardial injury in mice via the eNOS-NO-cGMP-PKG pathway

(A and B) Representative western blot images showing levels of eNOS and PKG in cardiac tissue. Data are expressed as mean \pm SEM; n = 4, *p < 0.05 vs. HTN group. **p < 0.01 vs. HTN group.

(C and D) Representative western blot images showing the expression of PDE5 in cardiac tissues. Data are expressed as mean \pm SEM; n = 4, **p < 0.01 vs. HTN group.

Exercise training improves hypertension by CACNA2D1

As shown in Figures 9A and 9B, 10 μ mol/L Ang II-induced MCMEC significantly increased cell proliferation after treatment with 1 μ mol/L Losartan for 48 h. MCMEC was transfected with OE (overexpression) CACNA2D1 and detected by western blot. The expression of CACNA2D1 protein in MCMEC in the OE group was significantly higher than that in the control group (Figure 9C). Western blot analysis was performed to detect the changes of related protein levels in MCMEC under different treatments. The results showed that Losartan did not improve Ang II-treated MCMEC by CACNA2D1 (Figures 7D and 7E).

Discussion

Physical exercise regulates blood pressure in several ways. However, exercise can promote improved cardiopulmonary function and increase blood output of the heart, so that blood circulates faster in the body and blood pressure increases. However, long-term exercise training can increase heart contractility and capacity and increase cardiac output more effectively to regulate blood pressure.²⁰ Furthermore, exercise can promote vasodilation by releasing neurotransmitters and hormones, such as nitric oxide and acetylcholine, thus lowering blood pressure.²¹ Long-term exercise training can also improve vascular endothelial function and increase the release of nitric oxide, promoting vascular dilation and lowering blood pressure.²² One of the pathophysiological reasons for hypertension is an increase in calcium ion concentration.²³ After transcriptome analysis and screening of the experimental samples, the two genes with the most obvious changes were identified. CACNA2D1 encodes the voltage-dependent calcium channel subunit α -2/ δ -1, which is one of the constituent units of calcium channel proteins and can promote calcium ion transport. ACTN2 is related to calcium ion transport, and its expression assists calcium ion transport. In the qPCR measurement results of hypertensive mice, the expression of both genes was higher; however, after exercise intervention, the expression decreased. This shows that the decrease in blood pressure in hypertensive mice is directly related to the decrease in calcium ion levels after the exercise intervention.

Transcriptomic analysis showed that the expression of CACNA2D1 was significantly changed in the experimental samples. CACNA2D1 gene is involved in encoding calcium ion channel protein α 2 δ -1, and overexpression of CACNA2D1 will affect the expression of α 2 δ -1 protein, thus affecting the normal transport of calcium ions and the concentration of calcium ions inside and outside the cell. Proteomic analysis showed that the expression of the three proteins changed significantly in the experimental samples. As a transmembrane glycoprotein, CTNNA3 participates in many cell biological processes, such as cell adhesion, cell proliferation, cell migration, and apoptosis.²⁴ Some studies have shown that the expression of CTNNA3 in vascular endothelial cells and smooth muscle cells is related to the regulation of vascular structure and function.²⁵ CTNNA3 is a calcium-dependent protein for its function. When the concentration of intracellular calcium ions increases, calcium ions will bind to the specific domain of CTNNA3, thus promoting the aggregation of this protein and the initiation of transmembrane signal transduction.²⁶ Increased calcium ion levels during hypertension may indicate that increased blood pressure is affected by CTNNA3. Furthermore, laminin is a kind of protein widely expressed in vascular endothelial cells and smooth muscle cells, and

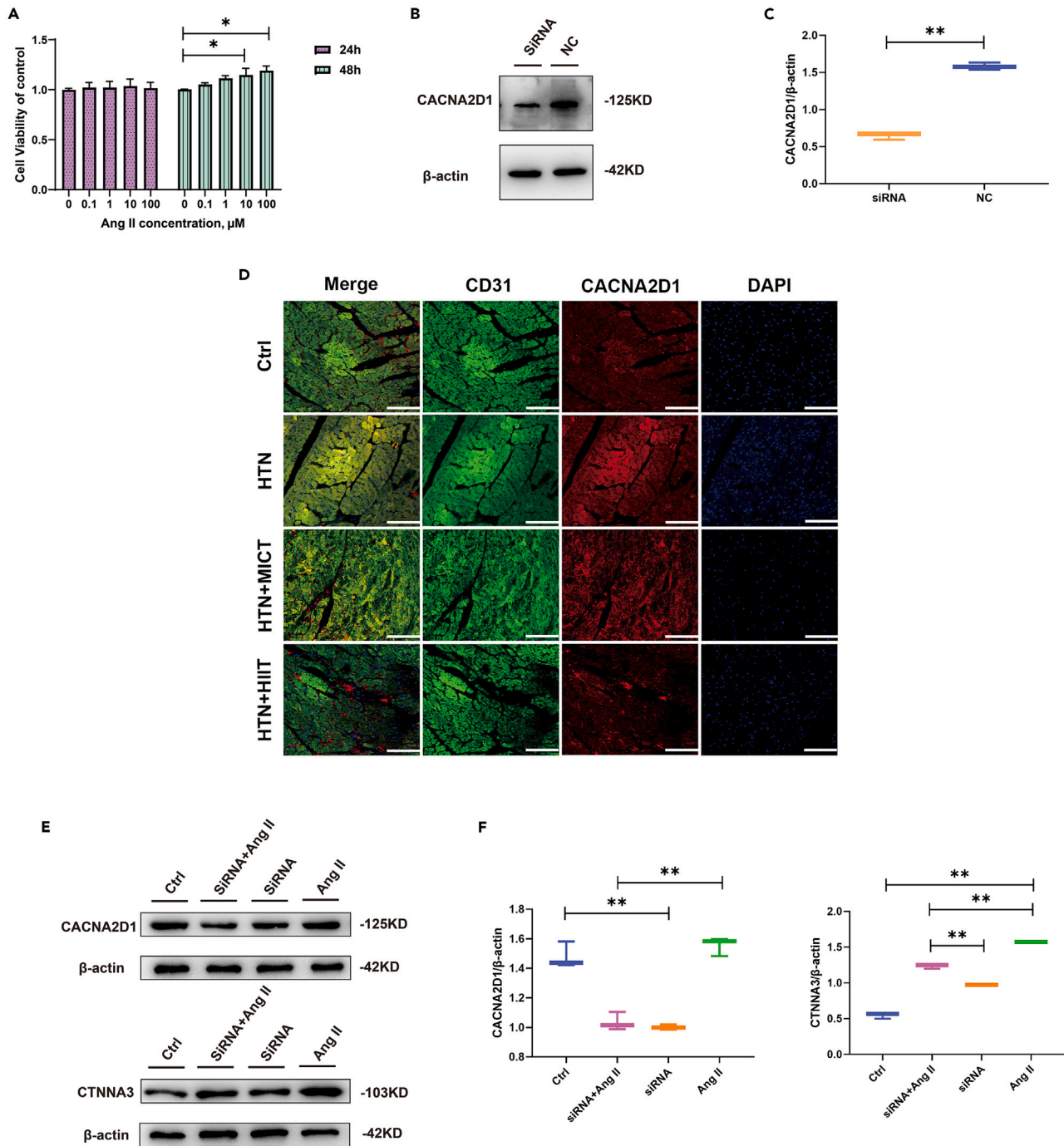


Figure 7. Downregulating CACNA2D1 regulated Ang II-treated MCMEC

(A) Effect of Ang II on MCMEC activity.

(B and C) MCMEC RNAi CACNA2D1 western blot results. Data are expressed as mean \pm SEM; n = 3, **p < 0.01 vs. NC group.

(D) CACNA2D1 was detected by immunofluorescence double labeling colocalization staining localization and expression of CD31 in left heart tissue of mice (scale = 100 μm).

(E and F) Representative western blot images showing the expression of CACNA2D1 and CTNNA3 in different treatments for MCMEC. Data are expressed as mean \pm SEM; n = 3, **p < 0.01 Ctrl group vs. Ang II group; Ctrl group vs. siRNA group; siRNA+Ang II group vs. siRNA group; siRNA+Ang II group vs. Ang II group.

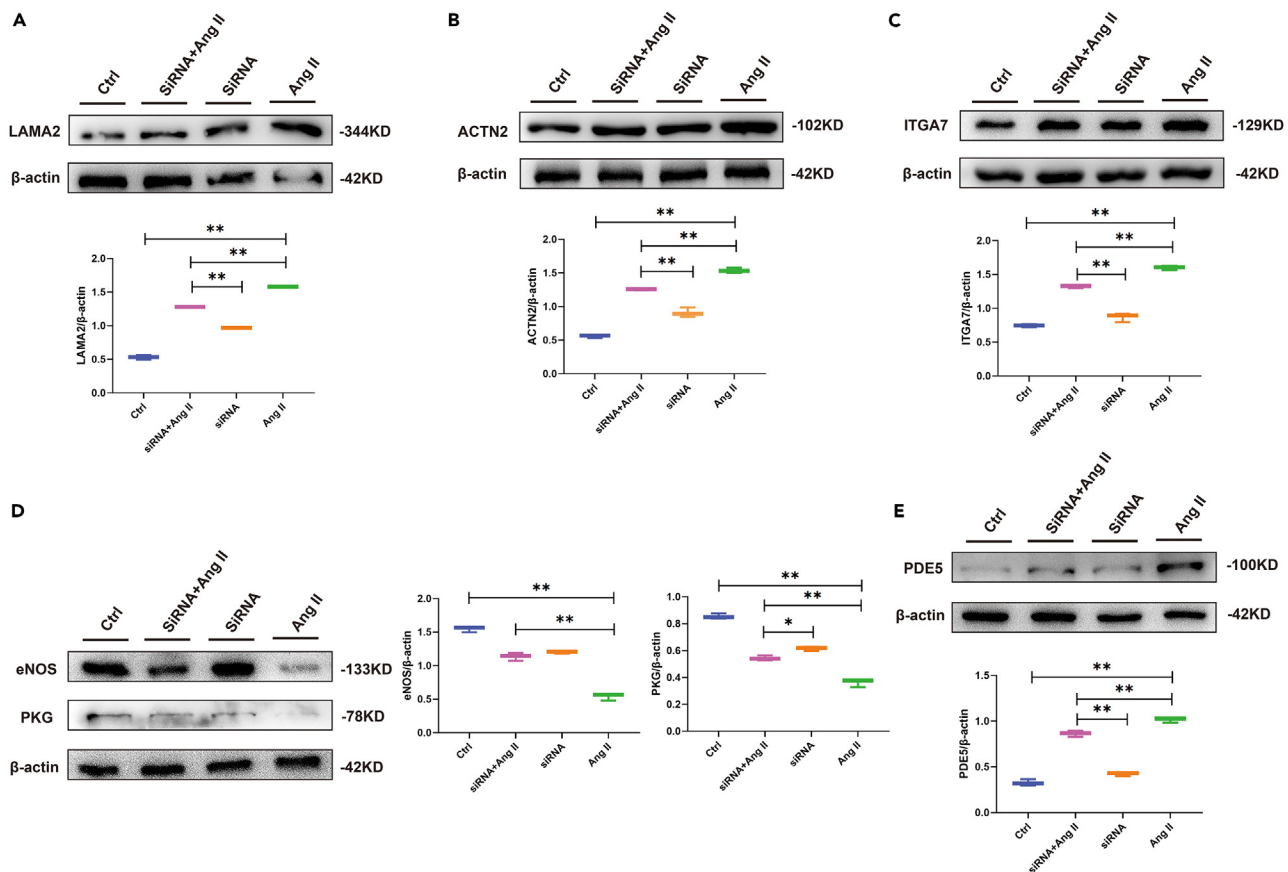


Figure 8. Downregulating CACNA2D1 can improve MCMEC injury after Ang II treatment

(A–C) Representative western blot images showing the expression of LAMA2, ACTN2, and ITGA7 in different treatments for MCMEC. Data are expressed as mean \pm SEM; $n = 3$, $**p < 0.01$ Ctrl group vs. Ang II group; siRNA+Ang II group vs. siRNA group; siRNA+Ang II group vs. Ang II group. (D and E) Representative western blot images showing the expression of eNOS, PKG, and PDE5 in different treatments for MCMEC. Data are expressed as mean \pm SEM; $n = 3$, $**p < 0.01$ Ctrl group vs. Ang II group; siRNA+Ang II group vs. siRNA group; siRNA+Ang II group vs. Ang II group.

its molecular structure contains numerous subunits, of which LAMA2 is a member.²⁷ Current research suggests that LAMA2 may be involved in the regulation of blood pressure. The expression level of LAMA2 has been found to change in patients with hypertension.²⁸ This suggests that a decrease in LAMA2 expression may be related to the development of hypertension. Calcium ions can also regulate protein activity and bind to the LAMA2 domain, thus changing its conformation and structure and affecting its function. An increase in calcium ion concentration can promote the aggregation of LAMA2 and the initiation of transmembrane signal transduction.²⁹ This study shows that high concentrations of calcium ions promote the expression of this protein and promote an increase in blood pressure. Studies have shown that ITGA7 may regulate the biological processes of the heart and blood vessels, thus affecting the regulation of blood pressure. For example, ITGA7 can regulate the contraction and relaxation of cardiac muscle cells and affect the contraction and relaxation functions of the heart.³⁰ Likewise, studies have shown that increasing the concentration of calcium ions can promote the activity of ITGA7, and increasing the concentration of exogenous calcium ions can promote the aggregation of ITGA7 and activation of signal transduction, thus affecting biological processes such as cell adhesion, migration, and invasion.³¹ This study showed that increased calcium ion levels promoted an increase in ITGA7 activity and blood pressure, and, after exercise intervention, the protein decreased with a decrease in blood pressure. Studies have demonstrated that the NO-cGMP-PKG signaling pathway plays a central role in the negative regulation of cardiovascular responses and their disorders by inhibiting Ca^{2+} dynamics.³² Therefore, we proceeded to validate this pathway, again demonstrating that exercise improves hypertension by affecting calcium ions. HIIT increased eNOS and PKG and inhibited PDE5. In addition, by silencing CACNA2D1 gene in primary MCMEC to construct a cell swelling model, the study confirmed that downregulating CACNA2D1 can regulate ANGII-treated MCMEC and can improve AngII-treated cell damage. This result demonstrated the role of CACNA2D1 in the regulation of hypertension by exercise.

In this study, we demonstrated that HIIT can significantly treat HTN in mice compared to MICT by downregulating CACNA2D1, reducing Ca^{2+} concentration, and dilating vascular smooth muscle, thus improving myocardial damage induced by hypertension in mice.

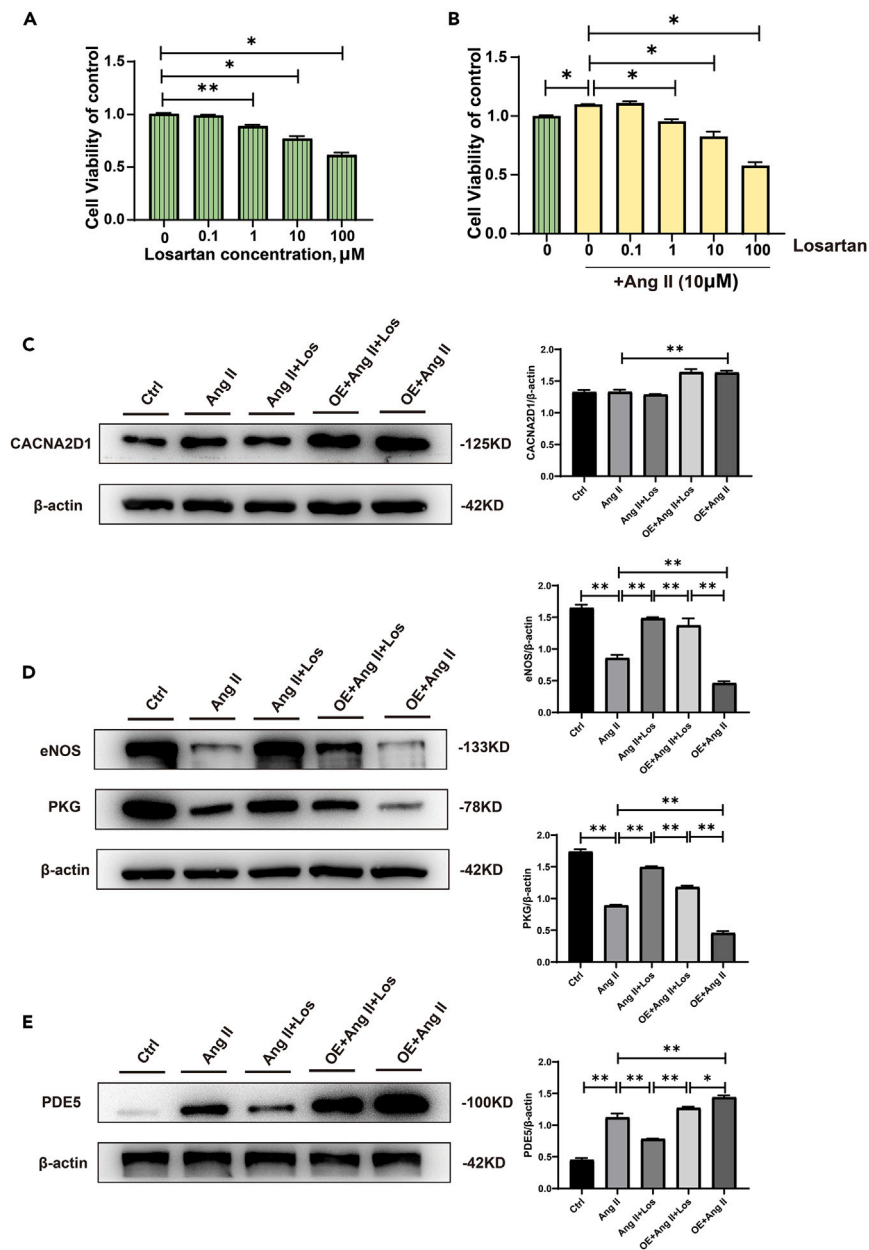


Figure 9. Exercise training improves hypertension by CACNA2D1

(A and B) Effect of Losartan on MCEC activity.

(C) Representative western blot images showing the expression of CACNA2D1 in different treatments for MCEC. Data are expressed as mean \pm SEM; n = 3, **p < 0.01 Ang II group vs. OE + Ang II group.

(D and E) Representative western blot images showing the expression of eNOS, PKG, and PDE5 in different treatments for MCEC. Data are expressed as mean \pm SEM; n = 3, *p < 0.05 OE + Ang II + Losartan group vs. OE + Ang II group; **p < 0.01 Ctrl group vs. Ang II group; Ang II group vs. Ang II + Losartan group; Ang II + Losartan group vs. OE + Ang II + Losartan group; OE + Ang II + Losartan group vs. OE + Ang II group; Ang II group vs. OE + Ang II.

Conclusions

In this study, we demonstrated that HIIT can significantly treat HTN mice compared to MICT in exercise therapy, by downregulating CACNA2D1, reducing Ca^{2+} concentration, and dilating vascular smooth muscle, thereby improving myocardial damage induced by hypertension in mice.

Limitations of the study

At present, we have not conducted more in-depth studies on calcium ions and calcium channels. *CACNA2D1* encodes calcium channel protein $\alpha_{2\delta-1}$, and overexpression of this gene will affect calcium channels and affect calcium ion concentration inside and outside cells. We will conduct further research on *CACNA2D1*, such as some calcium spark and channel activity detection experiments.

STAR★METHODS

Detailed methods are provided in the online version of this paper and include the following:

- **KEY RESOURCES TABLE**
- **RESOURCE AVAILABILITY**
 - Lead contact
 - Materials availability
 - Data and code availability
 - Experimental model and study participant details
- **METHOD DETAILS**
 - Exercise training regimen
 - Non-invasive blood pressure
 - Biochemical measurements
 - Histological staining
 - Proteomics
 - RNA-sequencing (RNA-seq)
 - Western blot
 - Cell extraction protein
 - MTS colorimetric method
 - Immunofluorescence
 - RNA interference (RNAi)
 - Quantitative real-time PCR
 - Immunohistochemistry
 - Cell overexpression (OE)
 - Statistical analysis

SUPPLEMENTAL INFORMATION

Supplemental information can be found online at <https://doi.org/10.1016/j.isci.2024.109351>.

ACKNOWLEDGMENTS

This work was supported by the Central Hospital of Dalian University of Technology “Climbing Plan” [grant number 2022ZZ226]. Sequencing service was provided by Personal Biotechnology Co., Ltd., Shanghai, China.

AUTHOR CONTRIBUTIONS

Z.P. designed the study; S.G., W.Y., and R.Z. carried out experiments; S.G. analyzed the data; S.G. drafted and wrote the manuscript; S.G. revised the manuscript; all authors read and approved the final manuscript.

DECLARATION OF INTERESTS

The authors declare no competing interests.

Received: October 1, 2023

Revised: December 26, 2023

Accepted: February 23, 2024

Published: February 28, 2024

REFERENCES

1. Manosroi, W., and Williams, G.H. (2019). Genetics of Human Primary Hypertension: Focus on Hormonal Mechanisms. *Endocr. Rev.* 40, 825–856. <https://doi.org/10.1210/er.2018-00071>.
2. Rossi, G.P., Bisogni, V., Rossitto, G., Maiolino, G., Cesari, M., Zhu, R., and Seccia, T.M. (2020). Practice Recommendations for Diagnosis and Treatment of the Most Common Forms of Secondary Hypertension. *High Blood Press. Cardiovasc. Prev.* 27, 547–560. <https://doi.org/10.1007/s40292-020-00415-9>.
3. Tziomalos, K. (2020). Secondary Hypertension: Novel Insights. *Curr.*

- Hypertens. Rev. 16, 11. <https://doi.org/10.2174/1573402115666190416161116>.
4. Elliott, W.J. (2007). Systemic hypertension. *Curr. Probl. Cardiol.* 32, 201–259. <https://doi.org/10.1016/j.cpcardiol.2007.01.002>.
 5. Sharman, J.E., Smart, N.A., Coombes, J.S., and Stowasser, M. (2019). Exercise and sport science australia position stand update on exercise and hypertension. *J. Hum. Hypertens.* 33, 837–843. <https://doi.org/10.1038/s41371-019-0266-z>.
 6. Moraes-Silva, I.C., Mostarda, C.T., Silva-Filho, A.C., and Irigoyen, M.C. (2017). Hypertension and Exercise Training: Evidence from Clinical Studies. *Adv. Exp. Med. Biol.* 1000, 65–84. https://doi.org/10.1007/978-981-10-4304-8_5.
 7. Malpas, S.C. (2010). Sympathetic nervous system overactivity and its role in the development of cardiovascular disease. *Physiol. Rev.* 90, 513–557. <https://doi.org/10.1152/physrev.00007.2009>.
 8. Oparil, S., Zaman, M.A., and Calhoun, D.A. (2003). Pathogenesis of hypertension. *Ann. Intern. Med.* 139, 761–776. <https://doi.org/10.7326/0003-4819-139-9-200311040-00011>.
 9. Polegato, B.F., and Paiva, S.A.R.d. (2018). Hypertension and Exercise: A Search for Mechanisms. *Arq. Bras. Cardiol.* 111, 180–181. <https://doi.org/10.5935/abc.20180146>.
 10. Börjesson, M., Onerup, A., Lundqvist, S., and Dahlöf, B. (2016). Physical activity and exercise lower blood pressure in individuals with hypertension: narrative review of 27 RCTs. *Br. J. Sports Med.* 50, 356–361. <https://doi.org/10.1136/bjsports-2015-095786>.
 11. Gorostegi-Anduaga, I., Corres, P., Martinez-Aguirre-Betolaza, A., Pérez-Asenjo, J., Aispuru, G.R., Fryer, S.M., and Maldonado-Martín, S. (2018). Effects of different aerobic exercise programmes with nutritional intervention in sedentary adults with overweight/obesity and hypertension: EXERDIET-HTA study. *Eur. J. Prev. Cardiol.* 25, 343–353. <https://doi.org/10.1177/2047487317749956>.
 12. Bannister, J.P., Bulley, S., Narayanan, D., Thomas-Gatewood, C., Luzny, P., Pachua, J., and Jaggar, J.H. (2012). Transcriptional upregulation of $\alpha 2\delta$ -1 elevates arterial smooth muscle cell voltage-dependent Ca^{2+} channel surface expression and cerebrovascular constriction in genetic hypertension. *Hypertension* 60, 1006–1015. <https://doi.org/10.1161/hypertensionaha.112.199661>.
 13. Sharman, J.E., La Gerche, A., and Coombes, J.S. (2015). Exercise and cardiovascular risk in patients with hypertension. *Am. J. Hypertens.* 28, 147–158. <https://doi.org/10.1093/ajh/hpu191>.
 14. Zhang, Y., Chen, Y., Xu, Z., Wu, Y., Zhang, Y., and Shi, L. (2020). Chronic exercise mediates epigenetic suppression of L-type Ca^{2+} channel and BKCa channel in mesenteric arteries of hypertensive rats. *J. Hypertens.* 38, 1763–1776. <https://doi.org/10.1097/hjh.0000000000002457>.
 15. Guan, W., Stephens, R.F., Mourad, O., Mehta, A., Fux, J., and Spafford, J.D. (2020). Unique cysteine-enriched, D2L5 and D4L6 extracellular loops in $\text{Ca}(\text{V})3$ T-type channels alter the passage and block of monovalent and divalent ions. *Sci. Rep.* 10, 12404. <https://doi.org/10.1038/s41598-020-69197-3>.
 16. Chen, J., Li, L., Chen, S.R., Chen, H., Xie, J.D., Sirrieh, R.E., MacLean, D.M., Zhang, Y., Zhou, M.H., Jayaraman, V., and Pan, H.L. (2018). The $\alpha 2\delta$ -1-NMDA Receptor Complex Is Critically Involved in Neuropathic Pain Development and Gabapentin Therapeutic Actions. *Cell Rep.* 22, 2307–2321. <https://doi.org/10.1016/j.celrep.2018.02.021>.
 17. Sabbahi, A., Arena, R., Elokda, A., and Phillips, S.A. (2016). Exercise and Hypertension: Uncovering the Mechanisms of Vascular Control. *Prog. Cardiovasc. Dis.* 59, 226–234. <https://doi.org/10.1016/j.pcad.2016.09.006>.
 18. Lopes, S., Félix, G., Mesquita-Bastos, J., Figueiredo, D., Oliveira, J., and Ribeiro, F. (2021). Determinants of exercise adherence and maintenance among patients with hypertension: a narrative review. *Rev. Cardiovasc. Med.* 22, 1271–1278. <https://doi.org/10.31083/j.rcm2204134>.
 19. Rodrigues, J.A., Primola-Gomes, T.N., Soares, L.L., Leal, T.F., Nóbrega, C., Pedrosa, D.L., Rezende, L.M.T., Oliveira, E.M.d., and Natali, A.J. (2018). Physical Exercise and Regulation of Intracellular Calcium in Cardiomyocytes of Hypertensive Rats. *Arq. Bras. Cardiol.* 111, 172–179. <https://doi.org/10.5935/abc.20180113>.
 20. Bove, A.A. (2016). Exercise and Heart Disease. *Methodist Debakey Cardiovasc. J.* 12, 74–75. <https://doi.org/10.14797/mdcj-12-2-74>.
 21. Cheng, T.L., Lin, Y.Y., Su, C.T., Hu, C.C., and Yang, A.L. (2016). Improvement of Acetylcholine-Induced Vasodilation by Acute Exercise in Ovariectomized Hypertensive Rats. *Chin. J. Physiol.* 59, 165–172. <https://doi.org/10.4077/cjp.2016.Bae387>.
 22. Oral, O. (2021). Nitric oxide and its role in exercise physiology. *J. Sports Med. Phys. Fit.* 61, 1208–1211. <https://doi.org/10.23736/s0022-4707.21.11640-8>.
 23. Shah, K., Seeley, S., Schulz, C., Fisher, J., and Gururaja Rao, S. (2022). Calcium Channels in the Heart: Disease States and Drugs. *Cells* 11. <https://doi.org/10.3390/cells11060943>.
 24. He, B., Li, T., Guan, L., Liu, F.E., Chen, X.M., Zhao, J., Lin, S., Liu, Z.Z., and Zhang, H.Q. (2016). CTNNA3 is a tumor suppressor in hepatocellular carcinomas and is inhibited by miR-425. *Oncotarget* 7, 8078–8089. <https://doi.org/10.18632/oncotarget.6978>.
 25. Nada, S., Kahaleh, B., and Altorok, N. (2022). Genome-wide DNA methylation pattern in systemic sclerosis microvascular endothelial cells: Identification of epigenetically affected key genes and pathways. *J. Scleroderma Relat. Disord.* 7, 71–81. <https://doi.org/10.1177/23971983211033772>.
 26. Liang, P., Zhu, W., Lan, T., and Tao, Q. (2018). Detection of salivary protein biomarkers of saliva secretion disorder in a primary Sjögren syndrome murine model. *J. Pharm. Biomed. Anal.* 154, 252–262. <https://doi.org/10.1016/j.jpba.2018.03.023>.
 27. Sarkozy, A., Foley, A.R., Zambon, A.A., Bönnemann, C.G., and Muntoni, F. (2020). LAMA2-Related Dystrophies: Clinical Phenotypes, Disease Biomarkers, and Clinical Trial Readiness. *Front. Mol. Neurosci.* 13, 123. <https://doi.org/10.3389/fnmol.2020.00123>.
 28. Meilleur, K.G., Linton, M.M., Fontana, J., Rutkowski, A., Elliott, J., Barton, M., McGraw, P., Kokkinis, A., Donkervoort, S., Leach, M., et al. (2017). Comparison of sitting and supine forced vital capacity in collagen VI-related dystrophy and laminin $\alpha 2$ -related dystrophy. *Pediatr. Pulmonol.* 52, 524–532. <https://doi.org/10.1002/ppul.23622>.
 29. Yanay, N., Elbaz, M., Konikov-Rozenman, J., Elgavish, S., Nevo, Y., Fellig, Y., Rabie, M., Mitrani-Rosenbaum, S., and Nevo, Y. (2019). Pax7, Pax3 and Mamstr genes are involved in skeletal muscle impaired regeneration of dy2J/dy2J mouse model of Lama2-CMD. *Hum. Mol. Genet.* 28, 3369–3390. <https://doi.org/10.1093/hmg/ddz180>.
 30. Bugiardini, E., Nunes, A.M., Oliveira-Santos, A., Dagda, M., Fontelonga, T.M., Barraza-Flores, P., Pittman, A.M., Morrow, J.M., Parton, M., Houlden, H., et al. (2022). Integrin $\alpha 7$ Mutations Are Associated With Adult-Onset Cardiac Dysfunction in Humans and Mice. *J. Am. Heart Assoc.* 11, e026494. <https://doi.org/10.1161/jaha.122.026494>.
 31. Häger, M., Bigotti, M.G., Meszaros, R., Carmignac, V., Holmberg, J., Allamand, V., Akerlund, M., Kalamajski, S., Brancaccio, A., Mayer, U., and Durbeej, M. (2008). Cib2 binds integrin $\alpha 7\beta 1$ and is reduced in laminin $\alpha 2$ chain-deficient muscular dystrophy. *J. Biol. Chem.* 283, 24760–24769. <https://doi.org/10.1074/jbc.M801166200>.
 32. Cai, Z., Wu, C., Xu, Y., Cai, J., Zhao, M., and Zu, L. (2023). The NO-cGMP-PKG Axis in HFpEF: From Pathological Mechanisms to Potential Therapies. *Aging Dis.* 14, 46–62. <https://doi.org/10.14336/ad.2022.0523>.

STAR★METHODS

KEY RESOURCES TABLE

REAGENT or RESOURCE	SOURCE	IDENTIFIER
Antibodies		
rabbit anti-eNOS	Proteintech	Cat# No. 27120-1-AP; RRID:AB_2880764
rabbit anti-NPPA	Proteintech	Cat# No. 27426-1-AP;RRID: AB_2880868
rabbit anti-BNP	Proteintech	Cat# No. 13299-1-AP; RRID:AB_2877935
rabbit anti-LAMA2	Proteintech	Cat# No. 23498-1-AP;RRID:AB_2879288
rabbit anti-CACNA2D1	Proteintech	Cat# No. 27453-1-AP; RRID:AB_2880874
rabbit anti-PRKG1	Proteintech	Cat# No. 21646-1-AP; RRID:AB_2878897
rabbit anti-ACTN2	Proteintech	Cat# No. 68223-1-Ig; RRID:AB_2935311
rabbit anti-ITGA7	Abcam	Cat# No.ab75224; RRID:AB_1310368
rabbit anti-PDE5A	Proteintech	Cat# No. 22624-1-AP; RRID:AB_2879137
HRP-conjugated Affinipure Goat Anti-Rabbit IgG(H + L)	Proteintech	Cat# No. SA00001-2; RRID:AB_2722564
HRP-conjugated Affinipure Goat Anti-Mouse IgG(H + L)	Proteintech	Cat# No. SA00001-1; RRID:AB_2722565
mouse anti-Beta Actin	Proteintech	Cat# No. 23660-1-AP; RRID:AB_2879307
mouse anti-CACNA2D1	Santa	Cat# No. sc-271697; RRID:AB_10708582
rabbit anti-CD31	Proteintech	Cat# No. 11265-1-AP; RRID:AB_2299349
rabbit anti-CTNNA3	Proteintech	Cat# No. 13974-1-AP; RRID:AB_2088078
Anti-rabbit IgG (H+L), F(ab') ₂ Fragment (Alexa Fluor® 488 Conjugate)	Cell Signaling Technology	Cat# No. 4412S; RRID:AB_1904025
Anti-mouse IgG (H+L), F(ab') ₂ Fragment (Alexa Fluor® 594 Conjugate)	Cell Signaling Technology	Cat# No. 8890S; RRID:AB_2714182
Critical commercial assays		
Calcium Assay Kit	Nanjing Jiancheng Bioengineering Institute	Cat# C004-2-1
Total RNA Kit(200)	Omega Bio-tek	Cat# R6834-02
Eastep™ qPCR Master Mix (2X)	Promega Technology	Cat# LS2062
Reverse Transcription System	Promega Technology	Cat# A3500
BCA kit	Shanghai -Beyotime Biotechnology	Cat# P6551
High Sensitivity DNA Kit	Agilent Technologies Inc.	Cat# 5067-4626
UltraSensitive™ SP (mouse/rabbit) IHC Kit	MXB Biotechnologies	Cat# 9720
CellTiter 96® AQueous Non-Radioactive Cell Proliferation Assay (MTS)	Promega Technology	Cat# G5421
Angiotensin II human (Ang II)	MedChemexpress Biotechnology Company	Cat# HY-13948
Losartan	MedChemexpress Biotechnology Company	Cat# HY-17512
Neofect DNA transfection reagents	Neofect	Cat# TF201201
Experimental models: Organisms/strains		
Mice: C57BL/6J	Liaoning Changsheng Biotechnology	N/A
Experimental models: Cell lines		
Mouse heart microvascular endothelial cells (MCMEC)	Shanghai Zhongqiao Xinzhou Biotechnology	Cat# PRI-MOU-00017
Oligonucleotides		
mCACNA2D1 oligo target sequences	Sangong Biotech	Table S1
plasmid vector CACNA2D1 target sequences	Sangong Biotech	Cat# H001
CTNNA3 primer sequences	invitrogen	Table S2

(Continued on next page)

Continued		
REAGENT or RESOURCE	SOURCE	IDENTIFIER
<i>Actn2</i> primer sequences	invitrogen	Table S2
<i>Cacna2d1</i> primer sequences	invitrogen	Table S2
<i>Lama2</i> primer sequences	invitrogen	Table S2
<i>Itga7</i> primer sequences	invitrogen	Table S2
Software and algorithms		
SPSS software version 23.0	SPSS software version 23.0	N/A
Adobe Photoshop CC 2019.Ink	Adobe Photoshop CC 2019.Ink	N/A
Adobe Illustrator 2022.Ink	Adobe Illustrator 2022.Ink	N/A
ImageJ.Ink	ImageJ.Ink	https://imagej.affinitycn.cn/
Microsoft Office Excel	Microsoft	https://www.microsoft.com
Deposited data		
raw sequence reads of the effect of exercise training on hypertension mice	NCBI (SRA)	Accession:PRJNA1077708
Other		
treadmill	Shanghai XinRuan Information Technology Co., Ltd.	No. XR-PT-10B
pressure Meter	Letica Scientific Instruments	LE 5001

RESOURCE AVAILABILITY

Lead contact

Requests for resources and reagents should be directed to the lead contact Zuowei Pei (pzw_dl@163.com).

Materials availability

All unique/stable reagents generated in this study are available from the [lead contact](#) with a completed Materials Transfer Agreement.

Data and code availability

Raw Sequencing data is deposited and publically available at the NCBI's Sequence Read Archive (SRA) with the project Accession: PRJNA1077708 , as listed in the [key resources table](#).

Any additional information required to reanalyse the data reported in this paper is available from the [lead contact](#) upon request. All data produced in this study are included in the supplementary information, or are available from the [lead contact](#) upon request.

Experimental model and study participant details

16-week-old male C57BL/6J mice were purchased from Liaoning Changsheng Biotechnology (Liaoning, China). Mice were housed in cages at 24–26°C, 40–60% humidity, and with a 12-hour light-dark cycle. Mice were randomly divided into: control group (n = 8), hypertension (HTN) group, n = 8, HTN + moderate intensity continuous exercise group (HTN + MICT group, n = 8), hypertension + high intensity intermittent exercise group (HTN + HIIT group, n = 8). With different treatments for each group, HTN by feeding 8% NaCl + AIN food (Xiao Shu You Tai (Beijing) Biotechnology Co., Ltd, Beijing, China) for 12 weeks (All procedures were approved by the Ethics Committee of Dalian Central Hospital [YN2022-039-33]). Our study lasted 10 weeks of an exercise training regimen, then at the end of the experiment, mice were anesthetized with 4% isoflurane through a nozzle placed on the nose, and blood samples from the eye sockets were collected from serum tubes and stored at –80°C until use. Mice were executed (1% sodium pentobarbital 60 mg/kg, intraperitoneally), followed by perfusion of mice through 0.9% saline. Blood samples were obtained from the abdominal aorta of the mice and collected in serum tubes, samples were stored at –80°C until use. When taking heart tissue, it is longitudinally divided into the left heart and the right heart. Then the left heart immobilized with 10% formalin and paraffin wax for histological observation. The right heart tissue was rapidly frozen in liquid nitrogen for Omics analysis, qPCR and western blot analysis.

METHOD DETAILS

Exercise training regimen

Mice running was performed on a treadmill (No. XR-PT-10B; Shanghai XinRuan Information Technology Co., Ltd. Shanghai, China), and \bar{V}_{max} of all exercising mice for the week was found by measuring V_{max} of each mouse once a week. V_{HIIT} was 85% of V_{max} , and the mice in the HIIT

group ran for 1.5 min resting for 1 min each time, for a total of 9 runs. The MICT group and the HIIT group kept the same total distance of exercise, and the V_{MICT} was V_{max} of 60%, to find out the total running duration, run the whole distance without rest at a uniform speed, All exercise mice ran five days per week.

Non-invasive blood pressure

Use a tail sleeve blood pressure Meter (LE 5001 pressure Meter; Leticia Scientific Instruments, Hospitalet, Spain), First, the mice were heated, placed on the fixator, and then the mice were placed in the incubator together with the fixator for measurement. The temperature of the incubator set at 25 ~ 32 ° C, and the use temperature is generally determined according to the pre-test results.

To measure, run the app and place the mice in the animal cage with its head turned inward and its tail exposed. Lift the pressure rod of the tail retainer, place the open tail side of the cage containing the mouse towards the air bag on the tail retainer, and press the cage with the pressure rod. Apply soapy water to the mice tail lead tube and guide the rat tail through the balloon side of the tail retainer and pull out the other end. Lift the pressure bar, move the cage as close to the retainer as possible, and straighten the tail so that the retainer balloon is located at the root of the tail. Place the pulse sensor in the holder and lift the tail while placing. The ventral side of the mice's tail is directly under the pulse sensor. Tighten the lever and hold down the animal cage. Gently press the rat tail on the pulse sensor, check the pressure of the tail pressure knob and the rat tail from the holder hole, and observe the waveform of the pulse channel until a good pulse signal is detected. After the normal pulse waveform was observed and recorded for at least 10 seconds, the tail sleeve was inflated and pressurized. When the pressure channel waveform rose, the pulse wave of the pulse channel gradually decreased to disappear, and the pulse wave of the pulse channel continued to be pressurized for about 20 mm Hg after the pulse wave disappeared. After 2 to 3 seconds, the air was deflated, the pressure dropped, and the pulse wave reappeared. After 10 seconds of complete recovery of pulse, the measurement was again inflated and deflated, and the measurement method was the same as above.

The measurements were repeated five times. According to the bushing pressure SBP when the blood flow is blocked, the pressure corresponding to the vanishing point of pulse wave is SBP. The pressure corresponding to the point at which the pulse wave begins to weaken is DBP.

The animals were trained for 5 days before starting the measurements to prevent stress, and the animals were preheated to 30°C with a heater. Blood pressure is measured several times between 8 a.m. and 11 a.m., and 10 consecutive blood pressure readings are considered acceptable. The measurements were preceded by three training sessions to acclimate the animals to the environment prior to baseline measurements and avoid stress responses that could affect vascular tone and resting blood pressure.

Biochemical measurements

Blood was collected and serum was prepared by centrifugation at 3000 rpm for 8 min, and the supernatant was used to determine Ca^{2+} (Nanjing Jiancheng Institute of Biological Engineering, Nanjing, China).

Histological staining

Heart tissue fixed in 10% buffered formalin was left overnight at 4°C, transferred to a descending ethanol series the next day (10 min each in 75%, 80%, 90%, 95%, and 100% ethanol), dehydrated in xylene (twice for 10 min each), and finally embedded in paraffin. Paraffin-embedded heart tissue sections with a continuous section thickness of 5 μm were taken, soaked in xylene (twice for 10 min each), dewaxed in a descending ethanol series (10 min each in 100%, 95%, 90%, 80%, and 75% ethanol), and finally washed in PBS (three times for 5 min each). Stained with hematoxylin-eosin staining (HE), Masson-trichrome staining and fitc-conjugated wheat germ agglutinin (WGA), respectively, and dehydrated in a rising ethanol series (10 min each in 75%, 80%, 90%, 95% and 100% ethanol) and xylene soaked (twice for 10 min each). Stains were sealed with neutral resin, air dried, and observed for histological changes. Images were acquired using a BX 40 vertical light microscope (Olympus, Tokyo, Japan).

Proteomics

Sample lysis and protein extraction utilized SDT (4% SDS, 100mM Tris-HCl, 1mM DTT, pH7.6) buffer. Visualization of protein bands was achieved through Coomassie Blue R-250 staining. LC-MS/MS analysis employed a Q Exactive mass spectrometer coupled to Easy nLC. The mass spectrometer operated in positive ion mode, and MS data were acquired using a data-dependent top10 method. Survey scans were acquired at a resolution of 70,000, and resolution for HCD spectra was set to 17,500. Normalized collision energy was set to 30 eV. Identification and quantitation of proteins Use MaxQuant 1.5.3.17 software to merge and search the original MS data of each sample for identification and quantitative analysis.

RNA-sequencing (RNA-seq)

For RNA-seq analysis, the concentration and purity were measured by Thermo Scientific NanoDrop2000 (Thermo Scientific, Waltham, Massachusetts, USA), Integrity is tested by Agilent 2100 Bioanalyzer (Agilent Technologies Inc, California, USA). PCR products were purified using AMPure XP beads to obtain the final library. Use Agilent 2100 Bioana (Agilent Technologies Inc, California, USA), The Agilent High Sensitivity DNA Kit (Agilent Technologies Inc., California, USA, 5067-4626) was conducted. Multiplexed DNA libraries are homogenized and mixed in equal volume. Will mix good text PE150 mode sequencing was performed on Illumina sequencers after the library was gradually diluted and quantified.

Western blot

Mice heart tissues frozen at -80°C were taken out, and appropriate tissue were placed in 1.5mL eppendorf (EP) tubes containing the pre-cooled mixture of protease phosphatase inhibitor. The tissues were cut up on ice, and then broken and cracked by ultrasound overnight to extract total proteins. Next day, the protein supernatant was collected by centrifugation at 12000 rpm in a centrifuge at 4°C for 40 minutes, absorb the supernatant into a new 1.5mL EP tube and measure its volume. The concentration of obtained protein and gradient standard protein samples (1, 0.5, 0.25, 0.125 and 0.0625 ng/ μL) was measured by BCA kit (Shanghai Beyotime Biotechnology) in 96-well plate. The OD value of 562nm was determined and the standard curve was calculated. Quantified into a new 1.5mL EP tube, boiling water bath for 5 minutes, stored at -80°C for later use. Protein samples were isolated using 10% sodium dodecyl sulfate-polyacrylamide gel electrophoresis (SDS-PAGE) and then transferred to polyvinylidene fluoride membranes (Immobilon, Millipore, Billerica, MA, USA). Seal the membrane at room temperature for 1 hour with 5% skim milk in TBST buffer (TBS contains 0.1% Tween-20) and incubate overnight with the following primary antibodies at 4°C : rabbit anti-eNOS (1:1000, Proteintech, Wuhan, China); rabbit anti- Natriuretic Peptide Precursor A (NPPA) (1:2000, Proteintech, Wuhan, China); rabbit anti- Brain natriuretic peptide (BNP) (1:500, Proteintech, Wuhan, China); rabbit anti-LAMA2 (1:1000, Proteintech, Wuhan, China), rabbit anti-CACNA2D1 (1:1000, Proteintech, Wuhan, China), rabbit anti-CTNNA3 (1:1000, Proteintech, Wuhan, China); rabbit anti-PKG (1:1000, Proteintech, Wuhan, China); rabbit anti-ACTN2 (1:10000, Proteintech, Wuhan, China); rabbit anti-ITGA7 (1:500, Abcam, Cambridge, UK); rabbit anti-PDE5A (1:2000, Proteintech, Wuhan, China). On day 2, TBST was cleaned (three times, 5 min each), followed by appropriate secondary antibody (Anti-Rabbit IgG, 1:5000; Anti-mouse IgG, 1:10000; Proteintech) for 1 h. Immunoreactive proteins were quantified using the NIH ImageJ software. mouse anti-Beta Actin (1:20000, Proteintech, Wuhan, China) was used as an internal control. Protein levels were normalized to those of Beta actin.

Cell extraction protein

Carefully vacuum the culture-medium with a negative press, using pre-cooled 0.1M. The Primary mouse heart microvascular endothelial cells (MCMEC) (Zhongqiao Xinzhou Biotechnology Co., LTD, Shanghai, China, PRI-MOU-00017) were washed twice with PBS and placed upright on ice for 2 min. 100 μL RIPA lysate (Cevin Innovation Biotechnology Co., LTD, Beijing, China, SW104-02) was added, and the cells were carefully scraped off the bottom of the petri dish using a cell scraper. All processes were performed on the ice. The suspended homogenate was transferred to a 1.5mL Ep tube for cracking on the ice for 30 min. After cracking, centrifuge at 13000 rpm at 4°C for 30 min. The cell protein supernatant was collected and transferred to a new 1.5mL Ep tube and stored in the refrigerator at -80°C for future use.

MTS colorimetric method

Logarithmic MCMEC was collected and cell suspension concentration was adjusted. After cell count, 100 μL cell suspension was added to the cell monolet covered with the bottom of the hole (96-well flat plate). The plate was adjusted to 8000 cells /100 μL , and the 96-well flat plate covered with cells was placed in 5% CO_2 . Incubate in a cell incubator at 37°C . On the second day, when the cells were attached to the wall, the culture medium in the pores was carefully sucked out after 4 h of serum-free culture, and Ang II (MedChemexpress Biotechnology Company, New Jersey, USA, HY-13948) solution with concentration gradient was added respectively. Incubate in a cell incubator for 48 h. Under dark environment, 20 μL MTS (Promega Biotechnology Co. LTD, Beijing, China, G3582) solution was added to each well and cultured in the cell incubator for 2 h. The light absorption values of each hole were measured at OD 490nm using a 96-well flat bottom plate taken from the cell vial incubator. The survival rate of cells treated with different concentrations of Ang II was calculated by formula.

The experiment was repeated three times and the data were analyzed statistically.

Immunofluorescence

Dewaxing of paraffin film, antigen repair, blocking and blocking are consistent with immunohistochemical procedures. Primary antibody incubation: mouse anti-CACNA2D1 (1:300, sc-271697, Santa, USA) and rabbit anti-CD31(1:300, 11265-1-AP, proteintech, Wuhan) antibodies were diluted proportionally in the same tube and dropped on tissues overnight at 4°C . After the primary antibody was removed, it was cleaned with PBS for 5 min, a total of 3 times. Under the condition of avoiding light, the corresponding fluorescent secondary antibody : Anti-rabbit IgG (H+L), F(ab')₂ Fragment (Alexa Fluor® 488 Conjugate) (1:300, 4412S, Cell Signaling Technology, Massachusetts, USA) and Anti-mouse IgG (H+L), F(ab')₂ Fragment (Alexa Fluor® 594 Conjugate) (1:300, 8890S, Cell Signaling Technology, Massachusetts, USA) of different colors was added, incubated at room temperature for 1 h, and cleaned with PBS for 5 min, a total of 3 times. DAPI (Servicebio Biotechnology Co., LTD, G1012)staining: under the condition of avoiding light, PBS was used to clean the cell nucleus for 5 min, 3 times; DAPI was used to stain the cell nucleus for 1min, and PBS was used to clean it for 5 min, a total of 3 times. The film was sealed with an anti-fluorescence quencher (Servicebio Biotechnology Co., LTD, G1401) and photographed by scanning under a confocal fluorescence microscope.

RNA interference (RNAi)

The cells were implanted in a 6 cm petri dish, and the cell density was about 60% when transfected. For small interfering RNA (siRNA) silencing, select the siRNA target sequence. Use according to manufacturer's instructions, the transfection kit of Shengong Bioengineering Co., Ltd. used CACNA2D1 siRNA to silence CACNA2D1 expression in MCMEC. Western blot verified the knockdown efficiency of CACNA2D1 in MCMEC. The siRNA target sequence is shown in [Table S1](#).

Quantitative real-time PCR

Total RNA was extracted from heart tissues using TRIzol reagent (Vazyme; R410-1). mRNA (1000 ng) was reverse transcribed into cDNA using MonScript™ RTIII All-in-One Mix (Monad; RN05003S). The primer sequences and the related SYBR Green probes are shown in [Table S2](#).

Immunohistochemistry

Embedding and deparaffinization steps are the same as those for histological staining. Citric acid/sodium citrate buffer (pH = 6) was boiled in a microwave oven on high heat for 3-5 min, and the tissue sections were immersed in the buffer on low heat for 1-2 min, removed and left at room temperature for 30 min to cool down, and washed in PBS (three times for 5 min each); blocked with peroxidase blocking agent added dropwise to the tissue for 10 min, and washed in PBS (three times for 5 min each); sheep serum was room temperature blocked for 1 hour, then incubated overnight at 4°C with the following primary antibodies: rabbit anti-CTNNA3 (1:300, Proteintech, Wuhan, China) and rabbit anti-CACNA2D1 (1:300, Proteintech, Wuhan, China). On the next day, the primary antibody was aspirated and washed in PBS (three times for 5 min each); the tissue was incubated dropwise for 1 h at room temperature with the secondary antibody (HRP-labeled goat anti-rabbit IgG) included in the N - Histofine Simple staining kit. Subsequently, the reaction was terminated by immersion in 3,3'-diaminobenzidine (Metal Enhanced DAB Substrate Kit; Cat. no. DA1015; Beijing Solarbio Science & Technology) for 10 min and then added to distilled water according to the manufacturer's instructions. Hematoxylin was re-stained for 1-2 min and rinsed under running water for 30 min; 1% hydrochloric acid alcohol was fractionated for 3 s and rinsed under running water for 3 min. Finally, stained sections were dehydrated in an ascending series of ethanol concentrations (10 min each for 75%, 80%, 90%, 95% and 100% ethanol) and xylene immersion (twice for 10 min each). The sections were sealed with neutral resin and dried naturally at room temperature. All sections were observed morphologically using an Olympus BX40 vertical light microscope (Olympus, Tokyo, Japan).

Cell overexpression (OE)

MCMEC cells were transfected with plasmid vector CACNA2D1 and empty vector as negative control construct NC-P, and overexpressed at the final concentration of 2.5 mg/L. Transfection was performed using Neofect DNA transfection reagents (TF201201; Neofect, Beijing) Manufacturer's manual. After transfection for 48 h., collection was used for protein extraction. The CACNA2D1 construct was generated by clone mouse CACNA2D1 cDNA into the pUC57 vector.(Sangong Biotech).

Statistical analysis

All data are expressed as mean \pm SEM. The data were statistically analyzed using SPSS software version 23.0 (SPSS Inc., Chicago, IL, USA). Variation between groups was analyzed by one-way ANOVA followed by Tukey's test. When $P < 0.05$ indicates a statistically significant difference.